Molecular Phylogenetics and Evolution 92 (2015) 155–164

Contents lists available at ScienceDirect

Molecular Phylogenetics and Evolution

journal homepage: www.elsevier.com/locate/ympev

A molecular genetic time scale demonstrates Cretaceous origins and multiple diversification rate shifts within the order Galliformes (Aves) ☆

R. Will Stein [a,*], Joseph W. Brown [b], Arne Ø. Mooers [a]

[a] Department of Biological Sciences, Simon Fraser University, Burnaby, BC V5A 1S6, Canada
[b] Department of Ecology and Evolutionary Biology, University of Michigan, Ann Arbor, MI 48109, USA

ARTICLE INFO

Article history:
Received 25 September 2014
Revised 19 May 2015
Accepted 11 June 2015
Available online 30 June 2015

Keywords:
Galliformes
Bayesian
Phylogeny
Fossil calibration
Diversification analysis
Mass extinction

ABSTRACT

The phylogeny of Galliformes (landfowl) has been studied extensively; however, the associated chronologies have been criticized recently due to misplaced or misidentified fossil calibrations. As a consequence, it is unclear whether any crown-group lineages arose in the Cretaceous and survived the Cretaceous–Paleogene (K–Pg; 65.5 Ma) mass extinction. Using Bayesian phylogenetic inference on an alignment spanning 14,539 bp of mitochondrial and nuclear DNA sequence data, four fossil calibrations, and a combination of uncorrelated lognormally distributed relaxed-clock and strict-clock models, we inferred a time-calibrated molecular phylogeny for 225 of the 291 extant Galliform taxa. These analyses suggest that crown Galliformes diversified in the Cretaceous and that three-stem lineages survived the K–Pg mass extinction. Ideally, characterizing the tempo and mode of diversification involves a taxonomically complete phylogenetic hypothesis. We used simple constraint structures to incorporate 66 data-deficient taxa and inferred the first taxon-complete phylogenetic hypothesis for the Galliformes. Diversification analyses conducted on 10,000 timetrees sampled from the posterior distribution of candidate trees show that the evolutionary history of the Galliformes is best explained by a rate-shift model including 1–3 clade-specific increases in diversification rate. We further show that the tempo and mode of diversification in the Galliformes conforms to a three-pulse model, with three-stem lineages arising in the Cretaceous and inter and intrafamilial diversification occurring after the K–Pg mass extinction, in the Paleocene–Eocene (65.5–33.9 Ma) or in association with the Eocene–Oligocene transition (33.9 Ma).

1. Introduction

Fossil evidence of neornithine (modern) birds from the Cretaceous is extremely limited, and this has hindered our understanding of the temporal origins of modern birds and the potential impact of the Cretaceous–Paleogene (K–Pg) mass extinction event (65.5 Mega annum (Ma)) on their diversification chronology (Dyke and van Tuinen, 2004). Early phylogenetic analyses reconstructing the evolutionary history of modern birds generated disparate chronologies, fueling a "rocks vs. clocks" debate over which type of data and methodology (strict fossil record vs. molecular sequence data calibrated with strict molecular clocks) should be used (Brown et al., 2007, 2008; Ericson et al., 2006, 2007). Donoghue and Benton (2007) argued for an approach where "rocks" provide minimum and "clocks" maximum age estimates for calibrated nodes, and two developments facilitated their suggested approach. The first was the development of Bayesian relaxed-clock methodologies (Drummond and Rambaut, 2007; Drummond et al., 2006) that include sophisticated and flexible

Abbreviations: AIC, Akaike information criterion; AGRP-i1&2, agouti-related protein gene introns 1 and 2; B-FIB-i7, beta-fibrinogen gene intron 7; BOLD, Barcode of Life Data; bp, base pairs; BEAST, Bayesian evolutionary analysis sampling trees; BEAUti, Bayesian evolutionary analysis utility; C-MOS, C-MOS proto oncogene; CO1, cytochrome oxidase 1 gene; CI, credibility interval; Cyt *b*, cytochrome *b* gene; DNA, deoxyribose nucleic acid; ESS, effective sample size; IOC, International Ornithological Committee; K–Pg, Cretaceous–Paleogene; LASER, likelihood analysis of speciation and extinction rates; Ma, mega annums; MCC, maximum clade credibility; MCMC, Markov chain Monte Carlo; MEDUSA, modeling evolutionary diversification using step-wise AIC; ND, dihydro nicotinamide adenine dinucleotide-ubiquinone oxidoreductase chain gene; OVO-i7, Ovomucoid gene intron 7; PAUP*, Phylogenetic analysis using parsimony*; RAxML, Randomized accelerated maximum likelihood; RDP-i1, Rhodopsin gene intron 1; S rDNA, subunit of ribosomal deoxyribose nucleic acid; SATé-II, Simultaneous alignment and tree estimation II; xml, extensible markup language.

☆ This paper was edited by the Associate Editor C. Krajewski.

* Corresponding author. Fax: +1 778 782 3496.
E-mail addresses: rwstein@sfu.ca (R.W. Stein), josephwb@umich.edu (J.W. Brown), amooers@sfu.ca (A.Ø. Mooers).

http://dx.doi.org/10.1016/j.ympev.2015.06.005
1055-7903/

means of temporal calibration (Ho and Phillips, 2009). The second was the discovery of two fossils that have clear affinities within extant neornithine orders and are dated either immediately before or immediately after the K–Pg boundary. *Vegavis iaai* is dated to the Late Cretaceous (66 Ma) and has affinities within crown Anseriformes (waterfowl; Clarke et al., 2005) and *Waimanu manneringi* is dated to the Early Paleogene (60.5 Ma) and has affinities with stem Sphenisciformes (penguins; Slack et al., 2006). These fossils, and the associated phylochronological reconstructions, provide evidence supporting a Cretaceous origin for modern birds (Jetz et al., 2012; Lee et al., 2014; Jarvis et al., 2014).

A Cretaceous split within the Galloanserae, between the Galliformes (landfowl) and the Anseriformes, is relatively uncontentious because *V. iaai* has phylogenetic affinities within crown Anseriformes (Clarke et al., 2005). Nevertheless, studies using Bayesian relaxed-clock methods and *V. iaai* as a calibration fossil provide disparate chronologies for the basal split in the Galloanserae (mean time to most recent common ancestor (tMRCA): 108 Ma, Crowe et al., 2006; 83 Ma, Haddrath and Baker, 2012; 66 Ma Jarvis et al., 2014). This is somewhat surprising because Galloanserae is one of the most consistently and highly supported clades in the avian phylogeny (Cracraft and Clarke, 2001; Ericson et al., 2006; Fain and Houde, 2004; Haddrath and Baker, 2012; Pacheco et al., 2011; Slack et al., 2006). In addition, divergence-time estimates for the Galliformes reported by Crowe et al. (2006), Pereira and Baker (2006b), and Dyke and van Tuinen (2004) have been criticized recently due to incorrect and (or) misplaced fossil calibrations that could bias overestimated divergence times (Ksepka, 2009; Mayr, 2008), and similar criticisms could be levied against more recent divergence chronologies for the Galliformes (e.g. Kan et al., 2010). Disparate chronologies within the Galliformes may be due to a combination of among-study variation in taxon sampling, fossil placement, calibration densities, amount and type of sequence data (mitochondrial and/or nuclear), and phylogenetic inference and dating methods. This suggests that detailed analyses within Galloanserae still offer promise for resolving whether diversification of the crown-group Galliformes commenced before or after the K–Pg mass extinction.

Although *V. iaai* indicates a Cretaceous origin for stem Galliformes, it remains unclear whether any lineages within crown Galliformes arose in the Cretaceous and survived the K–Pg mass extinction (Ksepka, 2009). Here, we use a large alignment of mitochondrial and nuclear DNA sequence data, fossil calibration and a combination of strict-clock and log-normally distributed uncorrelated relaxed-clock models to simultaneously reconstruct the phylogeny and diversification chronology of 225 of 291 (77%) extant Galliform taxa. This extensive taxon set includes representatives from each of the 5 families and from 75 of 84 (89%) recognized genera. The phylochronological reconstructions presented here were designed to: 1. Assess whether any lineages of crown Galliformes arose in the Cretaceous and survived the K–Pg mass extinction, and 2. Characterize the diversification dynamics of the Galliformes throughout their evolutionary history. van Tuinen et al. (2006) proposed a two-pulse model to account for the diversification chronology of modern non-passerine bird orders, with interordinal diversification in the Cretaceous and intraordinal diversification post-K–Pg, either early in the Paleogene (65.5–33.9 Ma) or in association with the Eocene–Oligocene transition (33.9 Ma). For the Galliformes specifically, van Tuinen et al. (2006) suggested a Cretaceous origin for the stem lineage followed by diversification of the crown group early in the Paleogene. Ideally, a taxonomically complete phylogenetic hypothesis should be used to characterize diversification dynamics, so we used taxonomic affinities to incorporate 66 data-deficient taxa and subsequently reanalyzed the DNA data matrix with data- deficient taxa included. These taxon-complete analyses generated a large distribution of candidate phylogenies that account for uncertainty in local topology and divergence times for data-deficient taxa. We used 10,000 candidate phylogenies sampled from this distribution to characterize diversification dynamics of the Galliformes and to assess whether their diversification chronology is consistent with the two-pulse model proposed by van Tuinen et al. (2006).

2. Materials and methods

2.1. Taxon set and taxonomic data

The Galliformes, as considered here, is composed of five families (Megapodiidae, Cracidae, Numididae, Odontophoridae and Phasianidae), 84 genera and 291 species (supplementary Table 1), and we used the most recent species accounts to specify the ingroup taxon set (del Hoyo et al., 1994; Delacour and Amadon, 2004; Jones et al., 1995). We selected four outgroup taxa from the Anseriformes, including representatives from each of the three families (Anatidae, Anhimidae and Anseranatidae; del Hoyo et al., 1992). We assigned taxon names based on the most recent version of the International Ornithologists Union's master list of bird names (IOC Master List version 3.3; Gill and Donsker, 2013). Due to the dynamic nature of taxonomy, we included seven additional ingroup taxa identified as distinct in recent molecular phylogenetic analyses and four putative ingroup taxa with DNA sequence data in GenBank (see supplementary materials for details and justifications). Together, these taxa comprise the taxon set and the taxonomic data used to include data-deficient taxa (see Section 2.3 below, supplementary Table 1 and supplementary materials).

2.2. DNA data matrix

We assembled a DNA data matrix from pre-existing GenBank and Barcode of Life Data (BOLD) System records (downloaded on or before July 31, 2012; supplementary Table 2). The matrix is composed of a novel set of 6 protein-coding (CO1, Cyt *b*, ND1, ND2, ND4 and ND5; 7827 bp; supplementary Tables 2 and 3) and 3 nonprotein-coding (control region, 12S and 16S rDNA; 2642 bp) mitochondrial loci together with 1 protein-coding (C-MOS; 587 bp) and 4 nonprotein-coding (AGRP-i1&2, B-FIB-i7, OVO-i7, RDP-i1; 3483 bp) nuclear loci. The matrix includes 225 of 291 (77%, including 75 of 84 recognized genera) ingroup taxa and 4 outgroup taxa. The matrix comprises 14,539 base pairs (bp) at its maximum extent; however, the alignment is sparse and taxonomic coverage is ~40% across loci (mitochondrial loci: 21–92%; nuclear loci 15–37%; supplementary Table 2). We did not adopt a 'total evidence' approach; instead we selected markers, particularly nuclear markers, with broad and complimentary taxonomic coverage (supplementary Table 2).

We aligned the sequence data from each locus with SATé-II (Liu et al., 2012) and removed start and stop codons from protein-coding sequences. Nonprotein-coding sequences are subject to high frequencies of insertions and deletions (in-dels), making some regions difficult to align confidently. Portions of the mitochondrial control region are prone to indels, so we excluded these previously identified hyper-variable domains (Crowe et al., 2006; Lucchini and Randi, 1999; Pereira et al., 2004). Consistent with this approach, we also excluded in-del rich regions from nonprotein-coding sequences. In these instances we aligned, edited and realigned the sequences in SATé-II until the alignment stabilized. We chose to partition the mitochondrial loci for two reasons: 1. some of the mitochondrial loci are protein-coding and some are nonprotein coding and 2. Shen et al. (2010) reported substantial variation among loci-specific Bremer support values for sub-partitions of the mitochondrion relative to a

mitochondrial-genome based phylogeny they inferred for the Phasianidae. We inferred the best-fit model of molecular evolution for each locus using MRMODELTEST2.0 (Nylander, 2004), PAUP*4.0 (Swofford, 2003) and AIC model selection criteria. Then we inferred individual gene trees in RAxML (Stamatakis, 2006), inspected the resulting topologies for consistency and conducted concatenated analyses in RAxML to assess topological support across the partitioned alignment.

Ideally, calibration fossils should have been included in a formal phylogenetic analysis or they should exhibit a diagnostic apomorphy (Parham et al., 2012); however, relatively few fossils attributable to Galloanserae meet these criteria (Ksepka, 2009). A notable exception is *V. iaai*, which has demonstrated phylogenetic affinities with stem Anatidae (Clarke et al., 2005). We therefore selected outgroup taxa to facilitate using *V. iaai* as a calibration fossil (Table 1). Due to the importance of calibrating the root node, we also followed Ksepka's (2009) recommendation to use *V. iaai* to calibrate the basal split within Galloanserae, between the Anseriformes and the Galliformes. A second notable exception is *Palaeortyx*, which exhibits a well-developed intermetacarpal process on the carpometacarpus (wing bone); this apomorphy is diagnostic of the clade uniting the Odontophoridae and the Phasianidae (Mayr, 2009). So, we used *Palaeortyx gallica* (Mayr et al., 2006), which is represented by a nearly complete articulated skeleton, to calibrate the node uniting the Numididae, the Odontophoridae and the Phasianidae. Finally, we selected two calibration fossils, *Boreortalis laesslei* (Brodkorb, 1954) and *Rhegminornis calobates* (Olson and Farrand, 1974), based on expert opinion. *B. laesslei* has historical affinities with *Ortalis* (Brodkorb, 1954; Cracraft, 1971), and we used it to calibrate crown Cracidae. *R. calobates* has historical affinities with Meleagridinae (Olson and Farrand, 1974) or with either Meleagridinae or Tetraoninae (Steadman, 1980), and we used it to calibrate the node uniting Meleagridinae and Tetraoninae. Until recently, *B. laesslei* was represented only by a partial tibiotarsus and partial humeri (leg bones) and *R. calobates* was represented only by a carpometacarpus. Recently, nearly complete skeletons have been assembled for both *B. laesslei* and *R. calobates* (Steadman, 2014, pers. com.). While *B. laesslei* and *R. calobates* do not formally meet the selection criteria of Parham et al. (2012), their historic affinities appear to be sound (Steadman 2014, pers. com.).

Following Ho and Phillips (2009), we used the minimum age of each fossil to set the hard minimum bound of a lognormal calibration density (Table 1), which is additionally characterized by a mean and standard deviation. For internal calibrations, we selected a mean that bounded 95% of the probability density within the 25-Ma interval preceding the fossil's minimum age and a standard deviation that split the probability density evenly across the midpoint of this interval (Table 1). We chose a 25-Ma interval because the basal node of Galliformes has been inferred to be ~100 Ma (Brown et al., 2008) and we used four fossils that are distributed temporally across the phylogeny. For the basal split within the Galloanserae, we selected a mean that bounded 95% of the probability density within a 44-Ma interval and a standard deviation that split the probability density evenly across the midpoint of this interval (Table 1). Here, we chose a 44 Ma interval because this corresponds to the difference between a recent estimate for the split (110 Ma) between the Anseriformes and the Galliformes (Brown et al., 2008) and the age of *V. iaai* (66 Ma; Clarke et al., 2005). The intervals bounding 95% of the probability density are wide, and thus should impose relatively weak age priors on calibrated nodes.

We used BEAST v1.6.1 (Drummond et al., 2006) to reconstruct the phylochronolgy of the Galliformes, and we used BEAUti v1.6.1 (Drummond and Rambaut, 2007) to generate BEAST input files. Here, we assigned substitution models, clock models, prior on node heights, topological constraints, calibration priors and MCMC specifications (Supplementary Table 1; Table 3.1). We used codon-position models (Shapiro et al., 2006) for protein-coding sequences. Codon-position models unlink the mutation rates of slower-evolving first and second codon positions from those of faster-evolving third positions, and this should help to partition the signal from protein-coding genes across the depth of the phylogeny. We tested rate constancy (molecular clock) with PAUP*4.0, and likelihood-ratio tests rejected a strict clock for all loci except the nuclear exon, C-MOS (df = 35, $p = 0.30$; all other loci: df = 43–209, $p \leqslant 0.0004$). So, we specified a strict-clock model for C-MOS and uncorrelated lognormally distributed relaxed-clock models for all other loci. Although the mitochondrial data is highly partitioned (9 loci and 9 partitions), the mitochondrion is inherited as a unit. So, we grouped all of the mitochondrial loci under a single relaxed-clock model; this reduces the number of clock-rates that need to be estimated. To facilitate temporal calibration, we set a birth–death prior on node heights and calibration priors based on our four dated fossils. In this same vein, we specified five topological constraints, four associated with fossil calibrations and one to enforce ingroup monophyly. Constrained nodes had high bootstrap support ($\geqslant$99%) in concatenated RAxML analysis (Table 1).

Table 1
Details of calibration fossils, calibrated nodes and calibration densities used in Bayesian phylochronological reconstructions for the Galliformes.

Fossil attributes and calibration parameters	*Vegavis iaai*		*Palaeortyx gallica*	*Boreortalis laesslei*	*Rhegminornis calobates*
Museum reference number	MLP 93-I-3-1[b]		PW2005/50 23a-LS[g]	PB743[a] PB2061[c] MCZ7068[c]	MCZ233I[i]
Validation	Phylogenetic analysis[b]		Apomorphy[f]	Expert opinion[k]	Expert opinion[k]
Reconciliation morphology and molecular data	NA		NA	NA	NA
Locality	Vegaland, Antarctica[b]		Enspel, Germany[g]	Gilchrist Co., Florida[a]	Gilchrist Co., Florida[i]
Stratigraphy and Age	Maastrichtian, Late Cretaceous[e]		Late Oligocene[h]	Early Miocene[l]	Early Miocene[l]
Calibrated node	Galloanserae crown[b]	Anseriformes crown[d]	Numididae-stem split[f]	Cracidae crown[j]	Meleagridinae and Tetraoninae crown[j]
Fig. 1 node label	A	B	E	H	R
Bootstrap support	NA	100	100	100	99
Hard minimum (Ma)	66.0	66.0	24.7	16.0	16.0
Soft maximum (Ma)	110.0	91.0	49.7	41.0	41.0
Mean lognormal density	3.09	2.52	2.52	2.52	2.52
Standard deviation lognormal density	0.42	0.42	0.42	0.42	0.42

Sources. [a] Brodkorb (1954), [b] Clarke et al. (2005), [c] Cracraft (1971), [d] Ksepka (2009), [e] Marenssi et al. (2001), [f] Mayr (2009), [g] Mayr et al. (2006), [h] Mertz et al. (2007), [i] Olson and Farrand (1974), [j] Steadman (1980), [k] Steadman (2014) pers. com, [l] White (1942).

To ensure that initial conditions did not bias results in our preliminary BEAST analyses, we conducted four 40-million step MCMC searches on three different starting trees, and each search was initiated with a different seed. We sampled the MCMC chain every 10,000 steps, discarded the first 15 million steps as burnin and combined the post-burnin sample of parameter estimates from each starting tree. This resulted in a sample of 10,000 trees and parameter estimates for each starting tree. We generated maximum clade credibility (MCC) trees using TREEANNOTATOR v1.6.1 and assessed convergence, mixing and effective sample size (ESS) using TRACER v1.6.0 (Rambaut and Drummond, 2012). Despite extensive MCMC searches, these preliminary analyses did not converge. The MCC trees and TRACER analyses suggested two potential problems. First, topological support was unexpectedly low within the Cracidae and the Phasianidae. Taxa with little sequence data contribute negligibly to the tree likelihood and, as a consequence, their affinities can be unstable. Inspection of the DNA data matrix revealed three taxa within the Cracidae (*Ortalis cinereiceps*, *Penelope albipennis* and *Penelope marail*) and five taxa within the Phasianidae (*Caloperdix oculeus*, *Galloperdix lunulata*, *Meleagris ocellata*, *Rhizothera longirostris* and *Tragopan melanocephalus*) with very limited sequence data (184–822 bp). We conducted additional RAxML analyses to assess the stability of these eight taxa, both individually and in combination with one another. These RAxML analyses identified six taxa (*O. cinereiceps*, *P. albipennis* and *P. marail, T. melanocephalus, G. lunulata*, *R. longirostris*) with unstable affinities. *G. lunulata* and *R. longirostris* are the only representative of their genus in the DNA data matrix; so, we developed simple constraint structures to facilitate their inclusion (see supplementary materials for details and justifications). The four remaining taxa with unstable affinities were treated as data-deficient and included in the taxon-complete analyses (see Section 2.3). Second, ESS values for three key parameters, posterior, tree likelihood and root height, were below the minimum ESS (100) indicative of sufficient posterior sampling and convergence. JWB diagnosed that this convergence problem was likely related to estimating several clock-rate parameters from a sparse DNA data matrix; this is a problem that is exacerbated by the MCMC algorithm's single parameter per-step updating.

Therefore, in addition to the specifications described above for the preliminary BEAST analyses, we extended the MCMC searches and modified the xml input files to resolve these problems. First, we excluded the four data-deficient taxa with unstable affinities. Second, we specified constraints to include *G. lunulata* and *R. longirostris*. Third, we introduced a compound parameter to facilitate simultaneous updating of clock rates. We then performed one 120-million step MCMC search for each starting tree and sampled the MCMC chain every 10,000 steps. We discarded the first 20-million steps as burnin, generated MCC trees in TREEANNOTATOR v1.6.1 and inspected parameter estimates in TRACER v1.6.0 to assess convergence, mixing and ESS values. The three analyses converged on similar topologies, chronologies and parameter estimates, and ESS values for three critical parameters, posterior (341–487), tree likelihood (943–1167) and root height (124–252), indicated adequate posterior sampling and that the individual analyses had converged. So, we combined 9999 post-burnin samples from each starting tree, which yielded a combined sample of 29,997 trees and associated parameter estimates. We uniformly thinned this combined sample back to 9999 trees and parameter estimates and generated a MCC tree in TREEANNOTATOR v1.6.1.

In a Bayesian analysis involving temporal calibration, it is critical to assess the contribution of the sequence data to the inferred chronology (Heled and Drummond, 2012); this can be done by comparing posterior estimates with expectations under the tree prior. The calibrated tree prior can be generated by simulating the tree prior on a fully constrained topology (Heled and Drummond, 2012), and this calibrated tree prior provides a critical benchmark for assessing the contribution of the sequence data to posterior node age estimates (Heled and Drummond, 2012). We generated the calibrated tree prior by simulating the tree prior on the MCC trees resulting from the final BEAST analyses of the DNA data matrix. To do this, we ran one 50 million-step MCMC search on each of the three MCC trees with topology fully constrained. We discarded the first 10 million steps as burnin and combined the remaining parameter estimates for summarization.

2.3. Taxon-complete analyses

Our taxon-complete analyses assign branch lengths to data-deficient taxa by exploiting the parameters of the birth–death model of node heights estimated from the sequence data. We used a two-step approach to accomplish this. First, we assigned the same substitution models, clock models, prior on node heights, topological constraints and calibration priors used in analyses of the DNA data matrix. Second, we generated simple taxonomic constraints to include 66 data-deficient taxa (four taxa with limited sequence data and unstable molecular affinities and 62 taxa with no sequence data (see supplementary methods for details and justifications)). To ensure a diverse sample of trees, we initiated separate MCMC searches with an incompletely resolved starting tree, which was resolved randomly in step 0 of the search. In total, we initiated 20,130-million step MCMC searches, specified a different initiation seed for each search, sampled the Markov chain every 100,000 steps, instead of every 10,000 steps, and discarded the first 30 million steps as burnin. Two of the starting trees were identical, so we excluded the results of one search. We combined 526 post-burnin samples from 13 searches and 527 post-burnin samples from 6 searches to generate a combined sample of 10,000 candidate trees and parameter estimates. We inspected this combined sample of parameter estimates in TRACER v1.6.0 to assess convergence, mixing and ESS values.

The BEAST input files used in these analyses and the phylogenetic hypothesis generated from the DNA data matrix have been submitted to Dryad (doi: 10.5061/dryad.p2pn8).

2.4. Diversification analyses

We conducted diversification analyses on the combined sample of 10,000 taxon-complete trees. More specifically, we compared the single-rate diversification models implemented in the R package LASER (Rabosky, 2006) with the rate-shift model implemented in MEDUSA (Alfaro et al., 2009; Brown et al., 2012; see Jetz et al., 2012 for a similar approach). LASER implements seven single-rate diversification models: pure birth, birth death, density dependent logistic, density dependent exponential, speciation variable (exponential speciation with constant extinction), extinction variable (constant speciation with exponential extinction), and speciation and extinction variable (exponential speciation and extinction). The rate-shift model implemented in MEDUSA allows pure-birth and birth–death to be modeled simultaneously on different parts of a single tree. LASER and MEDUSA use different likelihood equations, LASER reports AIC while MEDUSA reports AICc, and the AICc reported by MEDUSA is further penalized for the rate-shift parameter, even though it does not affect the likelihood (Alfaro et al., 2009). As a consequence, results from LASER and MEDUSA models cannot be compared directly. To facilitate comparison (following Jetz et al., 2012), we verified that the logLikelihoods from single rate pure-birth and birth–death models from LASER and MEDUSA differed consistently by a constant (1358.02) across a sample of 10 trees. Correcting for this difference and for the number of parameters estimated in each model

facilitated calculation of comparable AIC values for LASER and MEDUSA models.

3. Results

The phylochronological reconstructions based on the DNA data matrix for 225 ingroup and four outgroup taxa required the estimation of 143 parameters, which was accomplished through extensive MCMC sampling and three-replicate analyses. After combining the post-burnin samples of the three-replicate analyses, ESS values for three critical parameters, posterior (1171), tree likelihood (3199) and root height (560), indicated sufficient posterior sampling for parameter estimation. All of the remaining 140 parameters had ESS $\geqslant$236, but most were >1000, indicating that the analyses had converged.

Before assessing whether any lineages of crown Galliformes arose in the Cretaceous, we first confirmed that the inferred chronology did not simply reflect expectation under the priors. To do this, we compared the posterior-mean time to most recent common ancestor (tMRCA) and the associated 95% credibility interval (CI, which is the same as 95% highest probability density) for the 5-calibrated nodes with those simulated under the calibrated tree prior (Table 2). Three posterior-mean tMRCA and three 95% CIs for calibrated nodes differed markedly from those simulated under the calibrated tree prior. Posterior-mean tMRCA for Galloanserae-crown and Numididae-stem splits (Fig. 1, nodes "A" and "E", respectively) were 12.6 Ma (14.8%) and 9.6 Ma (20.3%) older than those simulated under the calibrated tree prior (Table 2). Conversely, posterior-mean tMRCA for crown Cracidae (Fig. 1, node "H") was 12.4 Ma (36.7%) younger than simulated under the calibrated tree prior (Table 2). The 95% CI for posterior-mean tMRCA for the Numididae-stem split, Cracidae crown, and Meleagridinae and Tetraoninae crown (Fig. 1, node R) were 10.8 Ma (41.7%), 18.7 Ma (77.9%) and 4.7 Ma (38.5%) narrower, respectively, than those simulated under the calibrated tree prior (Table 2). Although the DNA data matrix is quite sparse, these

Table 2
Comparison of posterior mean time to most recent common ancestor (tMRCA) and the associated 95% credibility interval (CI) for the five-calibrated nodes in our Bayesian phylochronology of the Galliformes. The comparison is between results derived from analysis of the DNA data matrix (225 ingroup and 4 outgroup taxa) and simulation of the calibrated-tree prior on the fully constrained maximum clade credibility tree generated from analysis of the DNA data matrix.

Parameter	Clade	Fig. 1 node label	Posterior[a] (Ma)	Calibrated-tree prior[b] (Ma)
tMRCA	Galloanserae	A	97.8	85.2
	Anseriformes crown	B	76.4	76.5
	Numididae-stem split	E	56.8	47.2
	Cracidae crown	H	21.4	33.8
	Meleagridinae & Tetraoninae	R	26.7	25.8
95% CI	Galloanserae	A	23.7	23.4
	Anseriformes crown	B	13.3	13.7
	Numididae-stem split	E	15.1	25.9
	Cracidae crown	H	5.3	24.0
	Meleagridinae & Tetraoninae	R	7.5	12.2

[a] Posterior is the tMRCA or 95% CI derived from the molecular data, fossil-calibration densities and birth–death prior on node heights.

[b] Calibrated-tree prior is the simulated calibration densities and birth–death prior on node heights on the topologically constrained maximum clade credibility tree resulting from analysis of the DNA data matrix.

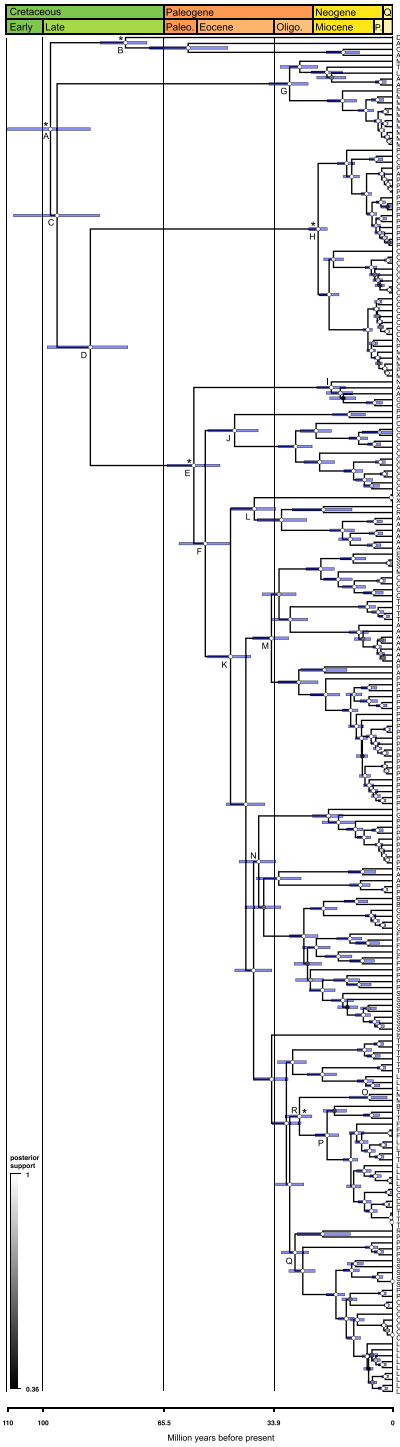

Fig. 1. Phylochronogy of 225 ingroup taxa from the Galliformes and 4 outgroup taxa from the Anseriformes derived from a concatenated analysis of a 14,539 bp alignment of mitochondrial and nuclear DNA sequence data. Calibrated nodes are indicated by an asterisk (*). Node bars represent the 95% credibility intervals for mean node age. The Cretaceous–Paleogene (65.5 Mega annums) and the Eocene–Oligocene (33.9 Mega annums) boundaries correspond to mass extinction events. "Pl." is an abbreviation for Pliocene and "Q." is an abbreviation for Quaternary. Nodes corresponding to recognized taxonomic levels are indicated by a capital letter: Super-ordinal (A: Gallonanserae), ordinal (B: Anseriformes, C: Galliformes), familial (G: Megapodiidae, H: Cracidae, I: Numididae, J: Odontophoridae, K: Phasianidae) and subfamilial (L: Arborophilinae, M: Coturnicinae, N: Pavoninae, O: Meleagridinae, P: Tetraoninae, Q: Phasianinae) stem splits. Capital letters along the backbone of the phylogeny correspond to family-level stem splits as follows: Megapodiidae-stem split (C), Cracidae-stem split (D), Numididae-stem split (E), and Odontophoridae- and Phasianidae-stem split (F).

comparisons show that the posterior rates of molecular evolution estimated from this matrix were influential in establishing the chronology presented here (Fig. 1).

Overall, the topology derived from the combined results of three replicate analyses of the DNA data matrix is well supported (Fig. 1). The divergence events forming the backbone of the phylogeny and leading to the 5 extant families, as well as the basal nodes of the five families, have either 1.0 posterior support (Supplementary Table 4), or, if constrained, 100% bootstrap support in concatenated RAxML analyses (Table 1). As a consequence, there is no topological uncertainty complicating our assessment of whether any extant Galliform lineages arose in the Cretaceous and survived the K–Pg mass extinction event (65.5 Ma). Five nodes are critical for making this assessment: the basal split in the Order, the Cracidae-stem split, the Numididae-stem split, crown Megapodiidae and crown Cracidae (Fig. 1, nodes "C", "D", "E", "G", and "H", respectively; Supplementary Table 4). The basal split in the Galliformes pre-dates the K–Pg boundary by >18 Ma (95% CI: 83.8–108.3 Ma; Fig. 1, node "C"). The Cracidae-stem split pre-dates the K–Pg boundary by >10 Ma (95% CI: 75.7–98.7 Ma; Fig. 1, node "D"). The Numididae-stem split post-dates the K–Pg boundary by $\geqslant$1.0 Ma (95% CI: 49.4–64.5 Ma; Fig. 1, node "E"). The Megapodiidae crown split post-dates the K–Pg boundary by $\geqslant$30 Ma (95% CI: 24.2–35.4 Ma; Fig. 1, node "G"). The Cracidae crown split post-dates the K–Pg boundary by >41 Ma (95% CI: 18.8–24.1 Ma; Fig. 1, node "H"). Our analyses strongly suggest that crown Galliformes diversified in the Cretaceous, that 3 extant lineages survived the K–Pg mass extinction and that all five of the family-level crown groups diversified after the K–Pg mass extinction.

ESS values for three critical parameters, posterior (2369), tree likelihood (6158) and root height (1611), estimated from the results of the taxon-complete analyses indicate sufficient posterior sampling for parameter estimation. All of the remaining 140 parameters had ESS $\geqslant$917, but most of these were >3000, indicating that the analyses had converged. Posterior-mean tMRCA from the taxon-complete analyses was 0.56 ± 0.13 Ma older, on average, than those from the DNA data matrix (Supplementary Table 5); including the 66 data-deficient taxa had little effect on the inferred chronology, as expected. Diversification analyses show that lineage accumulation leading to extant taxa stalled for ~30 Ma (86.4–56.8 Ma), resumed soon after the K–Pg mass extinction event and proceeded at a seemingly constant rate for ~40 Ma (Fig. 2). In an attempt to explain the whole-tree patterns of diversification, we used AIC model selection criteria to compete a set of 8 diversification models. All 7 of the single-rate diversification models implemented in LASER ran on all 10,000 trees except for the speciation-variable model, which failed to run on 924 trees. Among the 7 single-rate diversification models implemented in LASER, the speciation-variable model had the lowest AIC score on 9044 of the 9076 trees (99.6%) on which it ran (Table 3). The speciation-variable model is nested within the speciation-variable and extinction-variable model, and a likelihood ratio test performed on the results of the 9076 trees where the speciation-variable model ran shows that the simpler speciation-variable model was strongly preferred (mean ± standard error; difference in logLikelihood = 0.003 ± 0.001; p = 0.99 ± 0.00). The density dependent exponential and the speciation-variable models provided equally good fits to the data (mean ± standard error; ΔAIC = 1.28 ± 0.50). However, and importantly, MEDUSA's clade-specific rate-shift model out-performed LASER's speciation-variable model on 9999 of the 10,000 taxon-complete trees (Table 3; ΔAIC = 12.7 ± 0.2). MEDUSA analyses revealed substantial variation in mean diversification rate across the 10,000 trees and favored a combination of pure-birth and birth–death models for all trees (Fig. 3). Of the 10,000 trees analyzed, 64% exhibited one, 35% exhibited two and 1% exhibited three clade-specific increases in diversification rate.

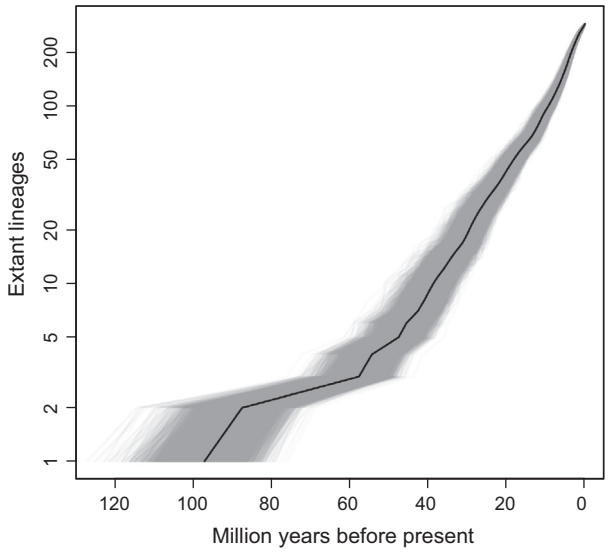

Fig. 2. Lineages through time plot for 10,000 taxon-complete candidate phylochronologies encompassing the entire evolutionary history of the Galliformes. Gray lines depict individual trees, and the black line represents the mean of these waiting times.

Table 3
AIC values for eight diversification models competed on 10,000 taxon-complete phylochronologies of the Galliformes. Likelihood values were standardized across analytical methodologies (MEDUSA and LASER) using the likelihood of the homogeneous birth–death model at its MEDUSA-based maximum likelihood parameter estimates.

Model	Model type	lnLK ± sem	AIC ± sem	ΔAIC ± sem
MEDUSA[a]	Clade shift	404.2 ± 0.2	1917.1 ± 0.4	00.0 ± 0.0
Speciation variable[b]	Temporal variation	398.4 ± 0.2	1925.1 ± 0.4	12.7 ± 0.2
Density dependent exponential	Temporal variation	394.7 ± 0.2	1930.5 ± 0.4	13.4 ± 0.0
Speciation and extinction variable	Temporal variation	396.4 ± 0.2	1931.2 ± 0.4	14.1 ± 0.0
Birth death	Constant-rate	392.5 ± 0.2	1935.1 ± 0.4	18.0 ± 0.0
Extinction variable	Temporal variation	392.4 ± 0.2	1937.2 ± 0.4	20.1 ± 0.0
Pure birth	Constant-rate	387.3 ± 0.2	1943.4 ± 0.4	26.3 ± 0.1
Density dependent logistic	Temporal variation	387.3 ± 0.2	1945.4 ± 0.4	28.3 ± 0.1

Abbreviations: lnLK is loglikelihood, AIC is Akaike information criterion and ΔAIC is change in Akaike information criterion.
[a] With 1–3 increases in diversification rate per tree.
[b] The speciation-variable model ran on 9076 of the 10,000 trees, and its ΔAIC value is based only on those 9076 trees.

4. Discussion

Although the Galliformes phylogeny has been relatively well studied, the timeline of evolution has been questioned recently and this has hindered characterization of diversification dynamics. As a consequence, the present investigation had two goals: 1. To test whether crown Galliformes originated in the Cretaceous; and 2. To characterize the full diversification dynamics of Galliformes. Achieving these goals was complicated by a combination of factors: the expected age (100 Ma) of the root node, a sparse DNA data matrix dominated by mitochondrial data, and the inclusion of 66 data-deficient taxa. Indeed, we encountered convergence problems

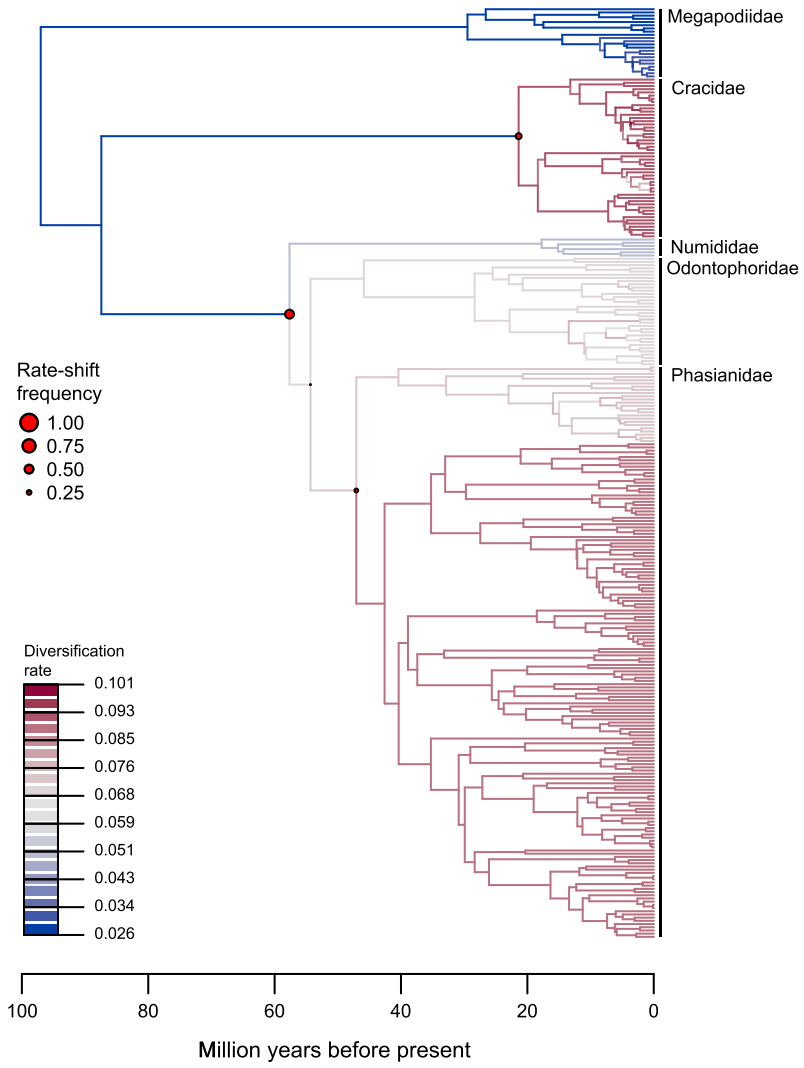

Fig. 3. Mean lineage-specific diversification rate and diversification-rate shifts inferred by MEDUSA on 10,000 taxon-complete candidate phylochronologies encompassing the entire evolutionary history of the Galliformes and mapped onto the taxon-complete maximum clade credibility tree.

in our preliminary BEAST analyses (see supplementary materials for an overview of the issues); however, after a careful and methodical diagnosis, we were able to remedy the causes of the problems prior to conducting our final analyses of the DNA data matrix and the taxon-complete analyses (see Sections 2.2 and 2.3, above). Based on a time-calibrated molecular phylogeny of 225 of 291 extant taxa, we show that crown Galliformes diversified in the Cretaceous (Fig. 1, node "C", 95% CI: 83.6–108.3 Ma), well before the K–Pg mass extinction (65.5 Ma), and that three extant lineages crossed the K–Pg mass extinction boundary (Supplementary Table 4). Diversification analyses conducted on 10,000 taxon-complete phylogenies demonstrate that lineage accumulation in the Galliformes was attenuated strongly coincident with the K–Pg mass extinction event (Fig. 2) and that the whole-tree pattern of lineage accumulation in the Galliformes was best explained by a rate-shift model including 1–3 clade-specific increases in diversification rate (Fig. 3). Our results suggest that the tempo and mode of diversification in the Galliformes conforms to a three-pulse, rather than a two-pulse, model governed by clade-specific rather than tree-wide variation. Such a "starburst" model of clade-specific diversification is reminiscent of recent patterns reported for birds as a whole (Jetz et al., 2012).

4.1. A molecular genetic timescale for the Galliformes

The most recent "large-scale" molecular phylogenetic hypotheses for the Galliformes have included only 30% (Wang et al., 2013) to 55% (Crowe et al., 2006) of extant taxa. These recent, large-scale molecular phylogenies of the Gallifomres recovered identical family-level affinities with high bootstrap support despite using non-overlapping sets of nuclear and only partially overlapping sets of mitochondrial loci (Crowe et al., 2006; Wang et al., 2013). The emerging consensus is Megapodiidae is sister to the four other families; Cracidae is sister to the clade uniting Numididae, Odontophoridae and Phasianidae; and Numididae is sister to Odontophoridae and Phasianidae. The time-calibrated molecular phylogeny of the Galliformes reported here (Fig. 1) is based on the most comprehensive taxon (225 of 291 species) and character (4070 bp nuclear and 10,469 bp mitochondrial DNA) sampling to date. Consistent with other recent large-scale molecular studies (Crowe et al., 2006; Wang et al., 2013), we recover identical family-level affinities with high posterior support. Due to a preponderance of short internodes, portions of the Galliformes phylogeny have proved difficult to resolve (Wang et al., 2013). Our DNA data matrix includes a novel set of nuclear exons and introns and an extensive set of mitochondrial protein-coding and non

protein-coding sequences selected to facilitate resolution across the depth of the phylogeny. Moreover, our analyses account for molecular rate variation among lineages, among loci and, for protein-coding loci, among codon positions. Consequently, our inferred phylogeny provides substantial additional resolution to the Galliformes phylogeny (Fig. 1, >80% of nodes have posterior support >0.95), and all of the short internodes forming the backbone of the phylogeny have posterior support $\geqslant 0.98$.

While an emerging consensus for the Galliformes phylogeny is gratifying, the timeline of their evolutionary history is more contentious (Ksepka, 2009). It is important, therefore, to compare the chronology derived from the posterior to the chronology simulated under the priors (Heled and Drummond, 2012). Our comparisons (Table 2) demonstrate marked deviations between posterior mean tMRCA and the 95% CIs inferred from the DNA data relative to expectation under the priors. Taken together, these results indicate that the inferred molecular rates were influential in setting the timeline of evolution reported here for the Galliformes.

Recent time-calibrated phylogenetic hypotheses for the Galliformes have consistently recovered a Cretaceous origin for crown Galliformes (Pereira and Baker, 2006a; Pereira and Baker, 2006b; Crowe et al., 2006); however, the results of these studies have been criticized due to the misidentification or misplacement of fossil calibrations, which could systematically bias older node age estimates (Ksepka, 2009). In the present study, we used *V. iaai* to calibrate crown Anserifomes, as originally suggested by Clarke et al. (2005). Following the recommendation of Ksepka (2009), we also used *V. iaai* to calibrate the divergence between the Anseriformes and the Galliformes (Galloanserae). Based on a apomorphy diagnostic of the clade uniting Odontophoridae and Phasianidae, we used *P. gallica* (Mayr et al., 2006) to calibrate the node uniting the Numididae, Odontophoridae and Phasianidae (Mayr, 2009). Although the phylogenetic affinities of the two additional fossils, *R. calobates* (Olson and Farrand, 1974), and *B. laesslei* (Brodkorb, 1954), that we selected based on expert opinion are less certain, there is no indication that their inclusion systematically biased older node age estimates (cf. Ksepka, 2009). Even in the most extreme case, where *B. laesslei* was used to calibrate crown Cracidae and the posterior mean tMRCA (21.4 Ma) was 37% younger and its 95% CI (18.8–24.1 Ma) was 78% narrower than expected under the priors, the 95% CI is symmetric around the posterior mean tMRCA. A symmetric, rather than a skewed, 95% CI suggests that the calibration density associated with *B. laesslei* did not systematically bias overestimation of posterior mean tMRCA in this case.

In a recent, large-scale study examining the diversification chronology of modern birds, Brown et al. (2008) inferred a time-calibrated molecular phylogeny for 27 orders, 100 families and 135 species, and limited their calibrations to fossils subjected to rigorous cladistic analyses. Sampling within the Galliformes was limited, but Brown et al. (2008) inferred that crown Galliformes diversified in the Cretaceous, 85–117 Ma ago, and that a second diversification event (76–110 Ma) occurred prior to the K–Pg boundary. We also inferred a Cretaceous origin for crown Galliformes (84–108 Ma ago) and a second diversification event (76–99 Ma) within crown Galliformes prior to the K–Pg boundary. Although the number of comparisons is limited, the mean tMRCAs inferred in the present study for stem Galliformes and for its family stem groups (Fig. 1, nodes "A", "C", "D", "E", and "F") are consistently younger (5–10 Ma) than those inferred by Brown et al. (2008); however, the 95% CIs are relatively wide (15–30 Ma) and overlap broadly. The present study corroborates the findings of Brown et al. (2008) and provides further evidence supporting a Cretaceous origin for crown Galliformes (Fig. 1 and Supplementary Table 4).

4.2. Diversification dynamics within the Galliformes

Diversification analyses ideally involve a taxonomically complete phylogenetic hypothesis. So, we used simple taxonomic constraint structures to incorporate 66 data-deficient taxa in a second series of phylogenetic analyses, and these analyses produced the first taxonomically complete phylogenetic hypothesis for the Galliformes. Including these 66 data-deficient taxa had a negligible impact on the inferred chronology (Supplementary Table 3). Diversification analyses conducted on 10,000 taxon-complete phylogenies demonstrate that the whole-tree pattern of lineage accumulation in the Galliformes was best explained by a model including 1–3 clade-specific increases in diversification rate (Fig. 3). A more thorough analysis is limited by the number of major clades represented in the present study and by the observation that families and geographic distribution are largely confounded. Below we highlight the potential importance of prehistoric human-induced extinction, colonization/dispersal, and sexual selection as factors that may account for our inferred clade-specific increases in diversification rate within the Galliformes.

Lineage accumulation in the Galliformes was attenuated strongly in association with the K–Pg mass extinction event (Fig. 2); as a consequence, the low and homogeneous diversification rates ($\sim$0.03 lineages $\times$ Ma^{-1}; Fig. 3) inferred for the three-stem lineages that arose in the Cretaceous and that crossed the K–Pg boundary are not surprising. However, we inferred a similarly low diversification rate ($\sim$0.03 lineages $\times$ Ma^{-1}; Fig. 3) for crown Megapodiidae (7 genera and 22 species), which diversified 24.3–35.5 Ma ago in the Oligocene (Fig. 1). The megapodes are confined to Indo-Australia, primarily to oceanic islands east of Wallace's line (Jones et al., 1995). Megapodes are relatively large (500–3000 g) ground-nesting birds with large, yolk-rich eggs and unique nesting behaviors (Jones et al., 1995), which would have made them an appealing and relatively easy food source for pre-historic people that colonized Oceania during the late Quaternary (Holocene/Anthropocene; 11,700 calendar yr before present; Steadman, 1999). The fossil record of megapodes from the late Quaternay is relatively sparse within their current geographic distribution; however, at least 7 extinctions have been documented during this period (Steadman, 1999). This led Steadman (1999) to suggest that >50% of megapode taxa may have gone extinct in association with pre-historic human colonization of Oceania. Given that extinction rates are notoriously difficult to estimate accurately from molecular phylogenies (Rabosky, 2010), we suggest that prehistoric anthropogenic-induced extinction may account, in part, for the low diversification rate inferred here for crown Megapodiidae.

MEDUSA analyses indicate that crown Cracidae (11 genera and 50 species) exhibited a burst of diversification during the Miocene and Pliocene, $\sim$23.0–2.5 Ma (Fig. 3). We inferred that crown Cracidae diversified 19.8–24.1 Ma ago in the late Oligocene – early Miocene (Fig. 1), which is appreciably more recent than previous estimates based on either limited mitochondrial (35–50 Ma ago; Pereira and Baker, 2006b) or more extensive mitochondrial and nuclear DNA sequence data (27–41 Ma ago; Pereira et al., 2002). Although the geographic distribution of crown Cracidae includes southern North, Central and South America (Delacour and Amadon, 2004), the majority of taxa are endemic to South America. Their current geographic distribution, in combination with inferred Gondwana origins, led to the suggestion that crown Cracidae diversified in South America (Pereira et al., 2002), while the scant fossil record suggests diversification commenced in North America (e.g., Brodkorb, 1954; Cracraft, 1971). The current and historical geographic distribution of crown Cracidae in combination with the diversification chronology presented here (Fig. 1),

suggest diversification in southern North America and subsequent colonization of South America via the Panamanian land bridge. South America presents a complex niche landscape, where vicariance events, such as marine transgression, uplift of the Andes and associated changes in river basins are all thought to have facilitated diversification of crown Cracidae (Pereira and Baker, 2004). Consistent with this, we suggest that crown Cracidae exhibited a rapid diversification when several lineages colonized South America ~4.5 Ma ago (Fig. 1).

MEDUSA analyses also indicated a sustained increase in diversification rate within the crown group uniting Numididae (4 genera and 6 species), Odontophoridae (10 genera and 34 species) and Phasianidae (52 genera and 178 species; Fig. 3). We inferred that this super-familial clade diversified 49.4–64.5 Ma ago in the Paleogene (Fig. 1), coincident with a period of climate warming 50–60 Ma ago that includes the Paleocene – Eocene thermal maximum (56 Ma; Zachos et al., 2008). This super-familial clade is distributed across all of the continents except Antarctica (del Hoyo et al., 1994). Crown Numididae (guineafowl) is restricted to coastal and sub-Saharan Africa (del Hoyo et al., 1994). Crown Odontophoridae (tooth-beaked quail) is distributed primarily across the Americas (del Hoyo et al., 1994); however, the genus *Ptilopachus* (two species), which is sister to all of the American Odontophorids, is also restricted to sub-Saharan Africa (Cohen et al., 2012). Crown Phasianidae (52 genera and 178 species) is distributed across Africa, Eurasia, Australia and North America (del Hoyo et al., 1994) and has been exceptionally successful at dispersing into a diverse set of terrestrial habitats. We inferred that Arborophilinae is sister to the five other subfamilies within Phasianidae, and that *Xenoperdix* (2 taxa) is sister to all other genera within Arborophilinae. Like Numididae and *Ptilopachus*, *Xenoperdix* is also restricted to a limited distribution in sub-Saharan Africa (Bowie and Fjeldå, 2005). This curious and consistent pattern of geographic distribution suggests the ancestor of this super-familial clade may have originated in Africa and that a sustained increase in diversification rate occurred in the context of long-distance dispersal and colonization. The Phasianidae is recognized as a model system for sexual selection (Darwin, 1871), and this suggests that sexual selection may have contributed to the sustained increase in diversification rate observed here (Seddon et al. 2013).

4.3. Tempo and mode of diversification in the Galliformes

The K–Pg mass extinction had a profound impact on the evolutionary history of birds (Longrich et al., 2011), and a subsequent, lesser mass extinction event marks the Eocene–Oligocene boundary (33.9 Ma; van Tuinen et al., 2006). Based on these mass-extinction events, van Tuinen et al. (2006) proposed a two-pulse model to account for the tempo and mode of diversification in modern, non-passerine birds. Specifically, van Tuinen et al. (2006) proposed ordinal diversification in the Cretaceous, producing a number of stem lineages that crossed the K–Pg boundary, and post-K–Pg diversification of crown-orders in association with either the Paleocene–Eocene thermal maximum (55 Ma ago) or the Eocene–Oligocene transition. Based on the mean tMRCA and the associated 95% CIs inferred here, we suggest that crown Galliformes diversified well before the K–Pg mass extinction event and that three-extant lineages crossed the K–Pg boundary (Fig. 1). One-stem lineage diversified in association with Paleocene–Eocene thermal maximum, giving rise to the super-familial clade uniting the Numididae, Odontophoridae and Phasianidae. This super familial-clade exhibited a sustained increase in diversification rate. Crown Megapodiidae and Crown Cracidea diversified at or after the Eocene–Oligocene transition. In contrast to the model proposed by van Tuinen et al. (2006), the tempo and mode of diversification for crown Galliformes appears to conform to a three-pulse, rather than a two-pulse, model. Our analyses suggest that the Eocene–Oligocene transition may have played a larger role in intra-familial diversification of the Galliformes than previously appreciated, and it may be that this is a more general phenomenon for non-passerine bird orders.

Acknowledgments

This contribution would not have been possible without the extensive previous work on the phylogeny of the Galliformes. We are particularly indebted to A.J. Baker, S.M. Birks, E.L. Braun, T.M. Crowe, S.V. Edwards, R.T. Kimball, N.J. Nadeau, S.L. Pereira and E. Randi for extensive sequencing and databasing efforts. In addition, we thank J.B. Joy for input on the phylogenetic and diversification analyses, G.J. Smith for assistance with managing numerous BEAST jobs to WestGrid, K.L. Parr for assistance with improving the quality of the figures and D. Steadman for in depth discussion on the fossil record of the Galliformes. This research was facilitated by the IRMACS Centre at SFU and supported by NSERC Canada through a PGS D scholarship to R.W. Stein and several Discovery grants to A.Ø. Mooers.

Appendix A. Supplementary material

Supplementary data associated with this article can be found, in the online version, at http://dx.doi.org/10.1016/j.ympev.2015.06.005.

References

Alfaro, M.E., Santini, F., Bock, C., Alamillo, H., Dornburg, A., Rabosky, D.L., Carnevale, G., Harmon, L.J., 2009. Nine exceptional radiations plus high turnover explain species diversity in jawed vertebrates. Proc. Natl. Acad. Sci. (USA) 106, 13410–13414.

Bowie, R.C.K., Fjeldå, J., 2005. Genetic and morphological evidence for two species in the Udzungwa forest partridge. J. East Afr. Nat. Hist. 94, 191–201.

Brodkorb, P., 1954. A chachalaca from the Miocene of Florida. Wilson Bull. 66, 180–183.

Brown, J.W., Payne, R.B., Mindell, D.P., 2007. Nuclear DNA does not reconcile 'rocks' and 'clocks' in Neoaves: a comment on Ericson et al. Biol. Lett. 3, 257–259.

Brown, J.W., Rest, J.S., Garcia-Moreno, J., Sorenson, M.D., Mindell, D.P., 2008. Strong mitochondrial DNA support for a Cretaceous origin of modern avian lineages. BMC Biol. 6, 6. http://dx.doi.org/10.1186/1741-7007-6-6.

Brown, J.W., FitzJohn, R.G., Alfaro, M.E., Harmon, L.J., 2012. MEDUSA: Modeling Evolutionary Diversification Using Stepwise AIC. <https://github.com/josephwb/turboMEDUSA>.

Clarke, J.A., Tambussi, C.P., Noriega, J.I., Erickson, G.M., Ketcham, R.A., 2005. Definitive fossil evidence for the extant avian radiation in the Cretaceous. Nature 433, 305–308.

Cohen, C., Wakeling, J.L., Mandiwana-Neudani, T.G., Sande, E., Dranzoa, C., Crowe, T.M., Bowie, R.C.K., 2012. Phylogenetic affinities of evolutionarily enigmatic African galliforms: the stone partridge *Ptilopachus petrosus* and Nahan's francolin *Francolinus nahani*, and support for their sister relationship with new world quails. Ibis 154, 768–780.

Cracraft, J., 1971. The humerus of the early Miocene cracid, *Boreortalis laesslei*. Wilson Bull. 83, 200–201.

Cracraft, J., Clarke, J., 2001. The basal clades of modern birds. In: Gauthier, J., Gall, L.F. (Eds.), Proceedings of the International Symposium in Honor of John H. Ostrom. Peabody Museum of Natural History, New Haven.

Crowe, T.M., Bowie, R.C.K., Bloomer, P., Mandiwana, T.G., Hedderson, T.A.J., Randi, E., Pereira, S.L., Wakeling, J., 2006. Phylogenetics, biogeography and classification of, and character evolution in, gamebirds (aves: galliformes): effects of character exclusion, data partitioning and missing data. Cladistics 22, 495–532.

Darwin, C., 1871. The Descent of Man, and Selection in Relation to Sex, vol. 1. John Murray, London.

del Hoyo, J., Elliot, A., Sargatal, J. (Eds.), 1992. Handbook of the birds of the world. Ostrich to Ducks, vol. 1. Lynx Edicions, Barcelona.

del Hoyo, J., Elliot, A., Sargatal, J. (Eds.), 1994. Handbook of the birds of the world. New World Vultures to Guineafowl, vol. 2. Lynx Edicions, Barcelona.

Delacour, J., Amadon, D., 2004. Curassows and Related Birds, second ed. Lynx Edicions and the National Museum of Natural History, Barcelona and New York.

Donoghue, P.C.J., Benton, M.J., 2007. Rocks and clocks: calibrating the tree of life using fossils and molecules. Trends Ecol. Evol. 22, 424–431.

Drummond, A.J., Rambaut, A., 2007. BEAST: Bayesian evolutionary analysis by sampling trees. BMC Evol. Biol. 7, 214. http://dx.doi.org/10.1186/1471-2148-7-214.

Drummond, A.J., Ho, S.Y.W., Phillips, M.J., Rambaut, A., 2006. Relaxed phylogenetics and dating with confidence. PLoS Biol. 4, e88. http://dx.doi.org/10.1371/journal.pbio.0040088.

Dyke, G.J., van Tuinen, M., 2004. The evolutionary radiation of modern birds (neornithes): reconciling molecules, morphology and the fossil record. Biol. J. Linn. Soc. 141, 153–177.

Ericson, P.G.P., Anderson, C.L., Britton, T., Elzanowski, A., Johansson, U.S., Källersjö, M., Ohlson, J.I., Parsons, T.J., Zuccon, D., Mayr, G., 2006. Diversification of neoaves: integration of molecular sequence data and fossils. Biol. Lett. 2, 543–547.

Ericson, P.G.P., Anderson, C.L., Mayr, G., 2007. Hangin' on to our rocks 'n clocks: a reply to Brown et al. Biol. Lett. 3, 260–261.

Fain, M.G., Houde, P., 2004. Parallel radiations in the primary clades of birds. Evolution 58, 2558–2573.

Gill, F., Donsker, D. (Eds.), 2013. IOC World Bird List (v 3.3). <http://www.worldbirdnames.org> (accessed 24.03.13).

Haddrath, O., Baker, A.J., 2012. Multiple nuclear genes and retroposons support vicariance and dispersal of the palaeognaths, and an early Cretaceous origin of modern birds. Proc. Royal. Soc. B 279, 4617–4625.

Heled, J., Drummond, A.J., 2012. Calibrated tree priors for relaxed phylogenetics and divergence time estimation. Syst. Biol. 61, 138–149.

Ho, S.Y.W., Phillips, M.J., 2009. Accounting for calibration uncertainty in phylogenetic estimation of evolutionary divergence times. Syst. Biol. 58, 367–380.

Jarvis, E.D., Mirarab, S., Aberer, A.J., Li, B., Houde, P., Li, C., Ho, S.Y.W., Faircloth, B.C., Nabholz, B., Howard, J.T., Suh, A., Weber, C.C., da Fonseca, R.R., Li, J., Zhang, F., Li, H., Zhou, L., Narula, N., Liu, L., Ganapathy, G., Boussau, B., Bayzid, Md S., Zavidovych, V., Subramanian, S., Gabaldón, T., Capella-Gutiérrez, S., Huerta-Cepas, L., Rekepalli, B., Munch, K., Schierup, M., Lindow, B., Warren, W.C., Ray, D., Green, R.E., Bruford, M.W., Zhan, X., Dixon, A., Li, S., Li, N., Huang, Y., Derryberry, E.P., Bertelsen, M.F., Sheldon, F.H., Brumfield, R.T., Mello, C.V., Lovell, P.V., Wirthlin, M., Paula Cruz Schneider, M., Prosdocimi, F., Alfredo Samaniego, J., Missael Vargas Velazquez, A., Alfaro-Núñez, A., Campos, P.F., Petersen, B., Sicheritz-Ponten, T., Pas, A., Bailey, T., Scofield, P., Bunce, M., Lambert, D.M., Zhou, Q., Perelman, P., Driskell, A.C., Shapiro, B., Xiong, Z., Zeng, Y., Liu, S., Li, Z., Liu, B., Wu, K., Xiao, J., Yinqi, X., Zheng, Q., Zhang, Y., Yang, H., Wang, J., Smeds, L., Rheindt, F.E., Braun, M., Fjeldsa, J., Orlando, L., Barker, F.K., Andreas Jønsson, K., Johnson, W., Koepfli, K., O'Brien, S., Haussler, D., Ryder, O.A., Rahbek, C., Willerslev, E., Graves, G.R., Glenn, T.C., McCormack, J., Burt, D., Ellegren, H., Alström, P., Edwards, S.V., Stamatakis, A., Mindell, D.P., Cracraft, J., Braun, E.L., Warnow, T., Jun, W., Gilbert, M.T.P., Zhang, G., 2014. Whole-genome analyses resolve early branches in the tree of life of modern birds. Sci. 346, 1320–1331.

Jetz, W., Thomas, G.H., Joy, J.B., Hartmann, K., Mooers, A.Ø., 2012. The global diversity of birds in space and time. Nature. http://dx.doi.org/10.1038/nature11631.

Jones, D.N., Dekker, R.W.R.J., Roselaar, C.S., 1995. The Megapodes. Oxford University Press, New York.

Kan, X., Li, X., Lei, Z., Chen, L., Gao, H., Yang, Z., Yang, J., Guo, Z., Yu, L., Zhang, L., Qian, C., 2010. Estimation of divergence times for major lineages of galliform birds: evidence from complete mitochondrial genome sequences. Afr. J. Biotechnol. 9, 3073–3078.

Ksepka, D.T., 2009. Broken gears in the avian molecular clock: new phylogenetic analyses support stem galliform status for *Gallinuloides wyomingensis* and rallid affinities for *Amitabha urbsinterdictensis*. Cladistics 25, 173–197.

Lee, M.S.Y., Cau, A., Naish, D., Dyke, G.J., 2014. Morphologocal clocks in palaeontology, and a mid-Cretaceous origin of crown aves. Syst. Biol. 63, 442–449.

Liu, K., Warnow, T., Holder, M.T., Nelesen, S., Yu, J., Stamatakis, A.P., Linder, C.R., 2012. SATé-II: very fast and accurate simultaneous estimation of multiple sequence alignments and phylogenetic trees. Syst. Biol. 61, 90–106.

Longrich, N.R., Tokaryk, T., Field, D.J., 2011. Mass extinction of birds at the Cretaceous–Paleogene (K–Pg) boundary. Proc. Nat. Acad. Sci. (USA) 106, 15253–15257.

Lucchini, V., Randi, E., 1999. Molecular evolution of the mtDNA control-region in galliform birds. In: Adams, N.J., Slotow, R.H. (Eds.), Proceedings of the 22 International Ornithological Congress, Durban. Birdlife South Africa, pp. 732–739.

Marenssi, S., Salani, S., Santillana, S., 2001. Geología de cabo Lamb, isla Vega, Antártida. Contrib. Inst. Antártico Argentino 530, 1–43.

Mayr, G., 2008. The fossil record of galliform birds: comments on Crowe et al. (2006). Cladistics 24, 74–78.

Mayr, G., 2009. Paleogene Fossil Birds. Springer-Verlag, Berlin. http://dx.doi.org/10.1007/978-3-540-89628-9, pp. 262.

Mayr, G., Poschmann, M., Wuttke, M., 2006. A nearly complete skeleton of the fossil galliform bird *Palaeortyx* from the late Oligocene of Germany. Acta Ornithol. 41, 129–135.

Mertz, D.F., Renne, P.R., Wuttke, M., Mödden, C., 2007. A numerically calibrated reference level (MP28) for the terrestrial mammal-based biozonation of the European upper Oligocene. Int. J. Earth Sci. 96, 353–361.

Nylander, J.A.A., 2004. MrModeltest v2. Program Distributed by the Author. Evolutionary Biology Centre, Uppsala University.

Olson, S.L., Farrand, J., 1974. *Rhegminornis* restudied: a tiny Miocene turkey. Wilson Bull. 86, 114–120.

Pacheco, M.A., Battistuzzi, F.U., Lentino, M., Aguilar, R.F., Kumar, S., Escalante, A.A., 2011. Evolution of modern birds revealed by mitogenomics: timing the radiation and origin of major orders. Mol. Biol. Evol. 28, 1927–1942.

Parham, J.F., Donoghue, P.C.J., Bell, C.J., Calway, T.D., Head, J.J., Holroyd, P.A., Inoue, J.G., Irmis, R.B., Joyce, W.G., Ksepka, D.T., Patané, J.S.L., Smith, N.D., Tarver, J.E., van Tuinen, M., Yang, Z., Angielczyk, K.D., Greenwood, J.M., Hipsley, C.A., Jacobs, L., Makovicky, P.J., Müller, J., Smith, K.T., Theodor, J.M., Warnock, R.C.M., Benton, M.J., 2012. Best practices for justifying fossil calibrations. Syst. Biol. 61, 346–359.

Pereira, S.L., Baker, A.J., 2004. Vicariant speciation of curassows (aves: cracidae): a hypothesis based on mitochondrial DNA phylogeny. Auk 121, 682–694.

Pereira, S.L., Baker, A.J., 2006a. A mitogenomic timescale for birds detects variable phylogenetic rates of molecular evolution and refutes the standard molecular clock. Mol. Biol. Evol. 23, 1731–1740.

Pereira, S.L., Baker, A.J., 2006b. A molecular timescale for galliform birds accounting for uncertainty in time estimates and heterogeneity of rates of DNA substitutions across lineages and sites. Mol. Phylogenet. Evol. 38, 499–509.

Pereira, S.L., Baker, A.J., Wajntal, A., 2002. Combined nuclear and mitochondrial DNA sequences resolve relationships within the cracidae (galliformes, aves). Syst. Biol. 51, 946–958.

Pereira, S.L., Grau, E.T., Wajntal, A., 2004. Molecular architecture and rates of DNA substitutions of the mitochondrial control region of cracid birds. Genome 47, 535–545.

Rabosky, D.L., 2006. LASER: a maximum likelihood toolkit for detecting temporal shifts in diversification rates from molecular phylogenies. Evol. Bioinforma. 2, 247–250.

Rabosky, D.L., 2010. Extinction rates should not be estimated from molecular phylogenies. Evolution 64, 1816–1824.

Rambaut, A., Drummond, A.J., 2012. Tracer v1.6.0. <http://beast.bio.ed.ac.uk/Tracer>.

Seddon, N., Botero, C.A., Tobias, J.A., Dunn, P.O., MacGregor, H.A.A., Rubenstein, D.R., Uy, J.A.C., Weir, J.T., Whittingham, L.A., Saffran, R.J., 2013. Sexual selection accelerates signal evolution during speciation in birds. Proc. Royal Soc., B 280, 20131065.

Shapiro, B., Rambaut, A., Drummond, A.J., 2006. Choosing appropriate substitution models for the phylogenetic analysis of protein-coding sequences. Mol. Biol. Evol. 23, 7–9.

Shen, Y., Liang, L., Sun, Y., Yue, B., Yang, X., Murphy, R.W., Zhang, Y., 2010. A mitogenomic perspective on the ancient, rapid radiation in the galliformes with an emphasis on the phasianidae. BMC Evol. Biol. 10, 155.

Slack, K.E., Jones, C.M., Ando, T., Harrison, G.L., Fordyce, R.E., Arnason, U., Penny, D., 2006. Early penguin fossils, plus mitochondrial genomes, calibrate avian evolution. Mol. Biol. Evol. 23, 1144–1155.

Stamatakis, A., 2006. RAxML-VI-HPC: maximum likelihood-based phylogenetic analyses with thousands of taxa and mixed models. Bioinformatics 22, 2688–2690.

Steadman, D.W., 1980. A review of the osteology and paleontology of turkeys (aves: meleagridinae). Contrib. Sci. Natur. Hist. Mus. Los Angeles County 330, 131–207.

Steadman, D.W., 1999. The biogeography and extinction of megapodes in Oceania. In: Dekker, R.W.R.J., Jones, D.N., Benshemesh, J. (Eds.), Proceedings of the Third International Megapode Symposium, Nhill, Australia, December 1997. Zoologische Verhandelingen, Leiden, 27, 7–21.

Swofford, D.L., 2003. PAUP*. Phylogenetic analysis using parsimony (* and other methods). Version 4. Sinauer Associates, Sunderland, Massachusetts.

van Tuinen, M., Stidham, T.A., Hadly, E.A., 2006. Tempo and mode of modern bird evolution observed with large-scale taxon sampling. Hist. Biol. 18, 205–221.

Wang, N., Kimball, R.T., Braun, E.L., Liang, B., Zhang, Z., 2013. Assessing phylogenetic relationships among galliformes: a multigene phylogeny with expanded taxon sampling in Phasianidae. PLoS ONE 8 (5), e64312. http://dx.doi.org/10.1371/journal.pone.0064312.

White, T.E., 1942. The lower Miocene mammal fauna of Florida. Bull. Museum Comp. Zool. 92, 1–49.

Zachos, J.C., Dickens, G.R., Zeebe, R.E., 2008. An early Cenozoic perspective on greenhouse warming and carbon-cycle dynamics. Nature 451, 279–283. http://dx.doi.org/10.1038/nature06588.